Energy Efficiency Method for RIS-Aided NOMA-SWIPT System

Zixuan Wang

School of Electronic Engineering and Information Technology, Sun Yat-Sen University, Guangzhou, China

Abstract. Due to the uncontrollability of the channel caused by the uncontrollability of the wireless transmission environment, the introduction of Reconfigurable intelligent surface (RIS) is needed to intelligently control the wireless propagation environment. We use RIS to improve the performance of non-orthogonal multiple access (NOMA)-based Simultaneous wireless information and power transfer (SWIPT) systems. This is done by maximizing the efficiency of energy transfer while ensuring the quality nature of NOMA-based information transmission. To achieve these objectives, we find the optimal phase shift of the RIS using the Semi-Definite Program (SDP) method and determine the optimal NOMA power distribution coefficient using a search approach. The simulation results demonstrate that our scheme improves the energy transfer efficiency compared to the conventional method without RIS.

Keywords: SWIPT, NOMA, RIS, resource allocation.

1. Introduction

In the development of the Internet of Things (IoT), there is a widespread need for low-power and low-cost IoT system. There must be a large number of sensors in future IoT system, and it needs massive data transmission. Simultaneous wireless information and power transfer (SWIPT) is considered to be a promising means of future communication [1][2]. In this way, the terminal can collect the energy of the radio frequency (RF) signal while receiving information, thereby improving the terminal 's endurance time, which has attracted wide attention from academia and industry. Typically, it is not feasible to execute both Energy Harvesting (EH) and Information Decoding (ID) procedures on a single incoming signal within a prompt system. This is because carrying out an EH process on a RF signal typically obliterates the informational integrity of the signal. In order to implement swift, it is necessary to differentiate the received signal, one way is to split the received signal in two, or use separate antennas on EH users and ID users. The receiver architecture of SWIPT includes independent receiver, time switching, power splitting and antenna switching architecture. [3] introduces a SWIPT technology based on joint subcarrier and power allocation in OFDM systems. The technology uses a joint optimization algorithm to allocate appropriate subcarriers and power, which can achieve wireless energy transfer while not affecting the quality of information transmission. In addition, a beamforming technology for SWIPT in two-way relay channels is discussed in [4]. The technology uses forwarding between two relay nodes to combine and process signals, and it transmit them to the receiving node, achieving SWIPT in wireless communication. SWIPT can solve the problem of energy consumption of 6G system, which is in line with the development concept of green IoT. [5] describes an IoT device based on a distributed antenna system that enables energy-efficient SWIPT by varying the transmit power and power distribution.

Non-orthogonal multiple access (NOMA) technology, which allows multiple signals to be transmitted into free space at the same carrier frequency, is a technique for improving spectral efficiency that has gained widespread interest in recent years. NOMA enables concurrent access to identical orthogonal resource blocks, such as frequency bands, time slots, and spatial directions, by multiple users. Generally, NOMA schemes can be implemented in two styles, power domain NOMA (PD-NOMA), code domain NOMA (CD-NOMA)[6]. Among them, the most widely used is power domain NOMA. Power domain NOMA distinguishes resource blocks only by the difference in signal power. The transmitter allocates different transmit power to each user according to the given power allocation principle. In order to improve spectrum efficiency, NOMA introduces

interference from multiple users, where the information about different users is transmitted on the same resource block, and the information about a single user is recovered by means of Successive Interference Cancellation (SIC) during demodulation. According to the strength of the received signal, the receiving device uses SIC to improve the decode performance. The SIC initially resolves the signal with a significant power difference, considering all other user signals as noise. Subsequently, the demodulated signal is deducted from the received signal. The signal continues to demodulate other signals, so users with better channel conditions can eliminate channel interference of users with poor channel conditions[7]. The system performance of NOMA and traditional orthogonal multiple access (OMA) is compared [8]. In [8], the throughput maximization problem considering user fairness is used in NOMA and OMA systems. And it designs an algorithm that considers the energy efficiency of each user, as well as the channel conditions and quality-of-service requirements of different users. The proposed NOMA-based algorithm outperforms existing solution in terms of energy efficiency and user fairness.

The transmission performance of NOMA and SWIPT is limited by channel conditions. In the process of communication, channel conditions are often determined. In the past, people tried to optimize at the transmitter to improve performance. However, with the development of metasurface, there is a technology that can change the channel conditions. Reconfigurable intelligent surface (RIS) as a promising technology may be applied to future 6G deployment. The reflection unit of RIS is a key component that enables the system to reflect the incident electromagnetic wave in a controllable manner. Specifically, an RIS is a planar surface composed of many tiny elements that can electronically control the reflection, refraction, and diffraction of the incident signal to achieve a specific direction of the outgoing signal. By manipulating the reflection coefficients of each element, the reflection unit can produce a constructive or destructive interference pattern, thereby steering the reflected beam towards the desired direction. [9] first analyzes the physical mechanism of RIS from a theoretical perspective and derives mathematical expressions of radiation and scattering fields. The proposed model was verified, demonstrating the potential applications of RIS. As the number of reflective units increases, RIS performance becomes better and better, and the synergy of overhead and performance can give the optimum solution for a particular usage scenario [10]. RIS differs from traditional amplify-and-forward relays in that it lacks signal processing capabilities; rather, it passively reflects the signal, resulting in greater energy efficiency. RIS can achieve effective EH in its vicinity by allowing intelligent signal reflection over large apertures, compensating for the high attenuation of RF signals over long distances. [11] proposes a method of enhancing wireless networks based on RIS technology, by using joint active and passive beamforming to optimize the system performance. Experimental results demonstrate that compared with traditional wireless networks, RIS-based wireless networks have higher data rates and lower power consumption, achieving efficient wireless communication in various environments. And RIS can be deployed on building surfaces, ceilings, etc., which can effectively solve the problem of obstacle blocking. [12] investigates the performance of RIS versus Decode-and-Forward (DF) in relaying with an obstacle blocking the line-of-sight link. In some cases, RIS can provide higher rates and better performance than DF.

In [13], the scenario of transmitting information and energy to cell users based on RIS and NOMA was discussed, and its performance was better than traditional schemes without RIS assistance. [14] considers the joint optimization of energy collection and uplink and downlink rates of SWIPT-based IoT nodes under the conditions of RIS and NOMA. In Systems based on RIS and SWIPT [15], joint optimization of the transmit precoder at the access point and the reflected phase shift of the RIS is deemed effective in maximizing the weighted sum power received by EH receivers. [16]enhances the performance of NOMA and synchronous transmission by using RIS in the process of SWIPT. A two-stage RIS is set up in this system, which has a superior achievable rate than traditional solutions. This paper focuses on the SWIPT communication scenario, and realizes separate information transmission and separate energy transmission from the base station

(BS) to the user with single antenna. Use RIS and NOMA in this scenario to discuss performance gains.

Our main contribution is the innovative use of RIS to assist the NOMA-based SWIPT system. We have used the SDP method to obtain the optimal phase shift of the RIS reflector unit. Simulations have demonstrated the improved energy transfer efficiency of our system compared to a conventional system without RIS.

In Section II, a new RIS assisted NOMA SWIPT model is proposed and we analyze the formulation of the problem. Section III shows our proposed method to solve the problem. Section IV introduces our simulation result. And it demonstrates that our model has better performance than the system without RIS. Our conclusion is shown in Section V.

2. System model and problem formulation

2.1 System Model

Fig. 1 shows the downlink transmission in a RIS-NOMA-SWIPT system. This scenario consists of one base station, one RIS, and three users (UE). Assume that BS and the users have only one antenna. UE 1 and UE 2 are a NOMA pair, and UE 3 is a power-consuming device. The BS transmits NOMA signals to UE 1 UE 2 while charging UE 3. In this case, UE 1 and UE 2 needs ID, and UE 3 needs EH.

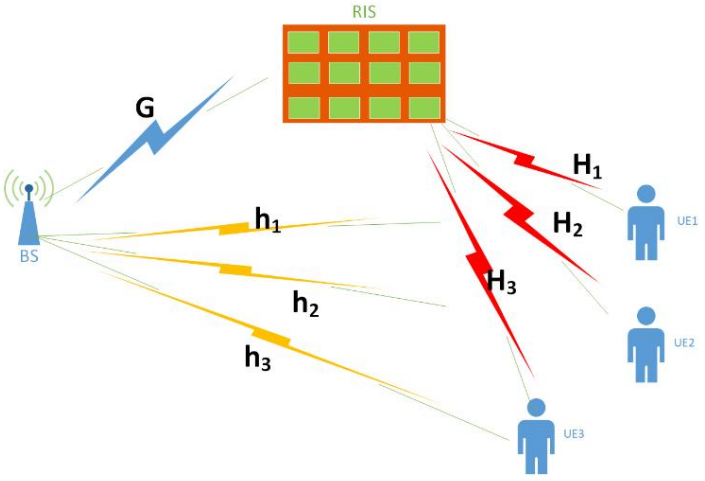

Fig. 1. System model

The RIS-user link behaves differently from the direct channel between the BS and the user. Specifically, each element of the RIS functions like a keyhole, combining all received multipath signals into a single physical point and re-scattering the combined signal as if it came from a point source [17]. Assuming that the RIS consists of N reflection modules, we use $\Theta = \mathrm{diag}\{\lambda_1 e^{j\theta_1}, \lambda_2 e^{j\theta_2}, \cdots, \lambda_N e^{j\theta_N}\}$ ($\mathrm{diag}(A)$ represents a diagonal matrix formed by taking the diagonal elements of matrix) to represent its reflection coefficient matrix, where $\lambda_n \in [0,1]$ and $\theta_n = \in [0,2\pi]$ are the amplitude reflection coefficient and the phase shift on the incident signal.

The baseband equivalent channels of BS-RIS link, RIS-UE k link are denoted by $G \in \mathbb{C}^{1\times N}$, $H_k \in \mathbb{C}^{N\times 1}$,respectively. Because the distance from BS to three users is different, the channel condition is also different, so we use h_1, h_2, h_3 to represent the BS to UE 1 channel, BS to UE 2 channel and BS to UE 3 channel. Then, the signal is transmitted through direct channel and indirect channel. The indirect BS-RIS-user channel can be modeled by BS-RIS link, RIS reflecting with phase shift, and RIS-user link.

We consider a downlink NOMA system. We only have one resource block(RB), and all of the user are assigned to this RB. The users in the same RB perform NOMA by allocating different power. So the transmitted signal by BS is

$$x = \sqrt{P_1}\cdot s_1 + \sqrt{P_2}\cdot s_2, \quad (1)$$

where s_1, s_2 is the signal for UE 1, UE 2, and they have normalized energy $E(|s|^2) = 1$. P_1 and P_2 denotes the transmit power assigned to the corresponding signal, which need to meet the following conditions,

$$P = P_1 + P_2, \quad (2)$$

where P is the total transmitted power of the BS. The received signal by UE 1 can be written as

$$y_1 = (G\cdot\Theta\cdot H_1 + h_1)\cdot(\sqrt{P_1}\cdot s_1 + \sqrt{P_2}\cdot s_2) + n_1, \quad (3)$$

where n_1 is the additive white Gaussian noise (AWGN) at the user receiver with zero mean and variance σ^2. For UE 1, it needs to demodulate the signal sent to UE 2 first and then demodulate the signal sent to itself. When demodulating UE 2 signal, UE 1 signal is considered as noise, so the received SINR for decoding the signal of s_2 can be written by

$$\gamma_{1\to 2} = \frac{P_2|G\cdot\Theta\cdot H_1 + h_1|^2}{P_1|G\cdot\Theta\cdot H_1 + h_1|^2 + \sigma^2}. \quad (4)$$

After SIC, the received SINR for decoding the signal of s_1 by UE 1 can be written by

$$\gamma_{1\to 1} = \frac{P_1|G\cdot\Theta\cdot H_1 + h_1|^2}{\sigma^2}, \quad (5)$$

The received signal by UE 2 can be written as

$$y_2 = (G\cdot\Theta\cdot H_2 + h_2)\cdot(\sqrt{P_1}\cdot s_1 + \sqrt{P_2}\cdot s_2) + n_2, \quad (6)$$

And the received SINR for decoding the signal of s_2 can be UE 2 written by

$$\gamma_{2\to 2} = \frac{P_2\cdot|G\cdot\Theta\cdot H_2 + h_2|^2}{P_1\cdot|G\cdot\Theta\cdot H_2 + h_2|^2 + \sigma^2}, \quad (7)$$

We use $\gamma_1, \gamma_2$to denote the required throughput. They satisfy $\gamma_{1\to 1} > \gamma_1, \gamma_{1\to 2} > \gamma_2, \gamma_{2\to 2} > \gamma_2$.

For the UE 3, the received signal from BS can be written as

$$y_3 = (G\cdot\Theta\cdot H_3 + h_3)\cdot(\sqrt{P_1}\cdot s_1 + \sqrt{P_2}\cdot s_2) + n_3, \quad (8)$$

Let E_3 denote the received power, then it can be written as

$$E_3 = |G\cdot\Theta\cdot H_3 + h_3|^2\cdot P, \quad (9)$$

2.2 Problem Formulation

To maximize the received power, we should jointly optimize P_1, P_2 and Θ. The optimized problem can be modeled as

$$(\mathrm{P1}) \max_{\Theta} \quad E_3, \quad (10a)$$

$$\text{s.t.} \quad |G\cdot\Theta\cdot H_1 + h_1|^2 > \frac{\gamma_1\sigma^2}{P1}, \quad (10b)$$

$$|G\cdot\Theta\cdot H_1 + h_1|^2 > \frac{\gamma_2\sigma^2}{P_2 - \gamma_2 P_1}, \quad (10c)$$

$$|G\cdot\Theta\cdot H_2 + h_2|^2 > \frac{\gamma_2\sigma^2}{P_2 - \gamma_2 P_1}, \quad (10d)$$

$$0 \le \theta_n \le 2\pi, \forall n = 1, \cdots, N, \quad (10e)$$

In the actual communication process, we do not want the amplitude of the signal to be attenuated, because this will have an impact on the subsequent demodulation and decoding. Although $\lambda_n \in [0,1]$, we set $\lambda_n = 1$, which ensures that the RIS maximize signal reflection.

In order for user k to successfully decode their information using SIC decoding, the SIC decoding constraints (10b)(10c)(10d) must be satisfied. These constraints are introduced by demodulating SINR(4)(5)(7). They ensure that the interference from other users is removed in the correct order during decoding, allowing each user to decode their information correctly.

3. Proposed Method

Problem (P1) is considered a non-convex optimization problem because of its non-concave objective function with respect to Θ. In this paper, by applying the Semidefinite Relaxation (SDR) algorithm, we propose a method to solve P1.

Let $v = [v_1, \cdots, v_N]^H$ where $v_n = e^{j\Theta_n}, \forall n$. Then, the constraints in (10e) equals to $|v_n| = 1, \forall n = 1, \cdots, N$. We make a variable conversion $G \cdot \Theta \cdot H_3 = v^H \Phi_3$, where $\Phi_3 = \mathrm{diag}(G)H_3$. So we have $|G \cdot \Theta \cdot H_3 + h_3|^2 = \| v^H \Phi_3 + h_3 \|^2$.Thus, problem(P1) equals to

$$(\mathrm{P2}) \max_{v} \quad v^H \Phi \Phi_3{}^H v + v^H \Phi_3 h_3{}^H + h_3 \Phi_3{}^H + h_3 h_3{}^H \tag{11a}$$

$$\text{s.t.} \quad |G \cdot \Theta \cdot H_1 + h_1|^2 > \frac{\gamma_1 \sigma^2}{P1}, \tag{11b}$$

$$|G \cdot \Theta \cdot H_1 + h_1|^2 > \frac{\gamma_2 \sigma^2}{P_2 - \gamma_2 P_1}, \tag{11c}$$

$$|G \cdot \Theta \cdot H_2 + h_2|^2 > \frac{\gamma_2 \sigma^2}{P_2 - \gamma_2 P_1}, \tag{11d}$$

$$|v_n| = 1, \forall n = 1, \cdots, N, \tag{11e}$$

Problem (P2) is a quadratically constrained quadratic program (QCQP) with respect to v, which can be transformed into a homogeneous QCQP. More precisely, the introduction of variable t enables us to express problem (P2) in an equivalent form as follows. When $t = 1$, P3 and P2 have the same form. For the problem of maximizing E_3, there is no effect on the solution of the problem when t is determined. The expression of constraint conditions (11b) - (11d) is consistent with the problem (P1), so we can use the same method to transform the constraint conditions.

Where

$$(\mathrm{P3}) \max_{v} \quad \bar{v}^H R_3 \bar{v}, \tag{12a}$$

$$\text{s.t.} \quad \bar{v_1}^H R_1 \bar{v_1} + h_1 h_1{}^H > \frac{\gamma_1 \sigma^2}{P1}, \tag{12b}$$

$$\bar{v_1}^H R_1 \bar{v_1} + h_1 h_1{}^H > \frac{\gamma_2 \sigma^2}{P_2 - \gamma_2 P_1}, \tag{12c}$$

$$\bar{v_2}^H R_2 \bar{v_2} + h_2 h_2{}^H > \frac{\gamma_2 \sigma^2}{P_2 - \gamma_2 P_1}, \tag{12d}$$

$$|\bar{v}_n| = 1, \forall n = 1, \cdots, N + 1, \tag{12e}$$

$$R_3 = \begin{bmatrix} \Phi_3 \Phi_3{}^H & \Phi_3 h_3{}^H \\ h_3 \Phi_3{}^H & 0 \end{bmatrix}, \tag{13a}$$

$$R_1 = \begin{bmatrix} \Phi_1 \Phi_1{}^H & \Phi_1 h_1{}^H \\ h_1 \Phi_1{}^H & 0 \end{bmatrix}, \tag{13b}$$

$$R_2 = \begin{bmatrix} \Phi_2 \Phi_2{}^H & \Phi_2 h_2{}^H \\ h_2 \Phi_2{}^H & 0 \end{bmatrix}, \tag{13c}$$

$$\bar{v} = \begin{bmatrix} v \\ t \end{bmatrix}, \tag{13d}$$

However, problem (P3) is NP-hard, which requires exponential levels of time to solve, and is not compatible in instant communication systems. So we need to further optimize its solution complexity. Note that $\bar{v}^H R \bar{v} = \mathrm{tr}(R \bar{v} \bar{v}^H)$. Define $V = \bar{v} \bar{v}^H$, which needs to satisfy $V \succcurlyeq 0$ and $\mathrm{rank}(V) = 1$. As the rank-one constraint is non-convex, we utilize SDR to relax this restraint. This results in problem (P3) being transformed into

$$(P4)\ \max_{V} \quad \mathrm{tr}(R_3 V), \tag{14a}$$

$$s.t. \quad V_{n,n} = 1, \forall n = 1, \cdots, N+1, \tag{14b}$$

$$V \succcurlyeq 0, \tag{14c}$$

$$\mathrm{tr}(R_1 V) + h_1 h_1^{H} > \frac{\gamma_1 \sigma^2}{P1}, \tag{14d}$$

$$\mathrm{tr}(R_1 V) + h_1 h_1^{H} > \frac{\gamma_2 \sigma^2}{P_2 - \gamma_2 P_1}, \tag{14e}$$

$$\mathrm{tr}(R_2 V) + h_2 h_2^{H} > \frac{\gamma_2 \sigma^2}{P_2 - \gamma_2 P_1}, \tag{14g}$$

The problem (P4) is a typical SDP and can be solved using existing convex optimization solvers like CVX[18]. To obtain a rank-one solution for problem (P4), additional steps are required to construct it from the optimal higher-rank solution. The eigenvalue decomposition of V as $V = U\Sigma U^{H}$ is obtained. Σ is the diagonal matrix whose elements on the diagonal are the corresponding eigenvalues , i.e. $\Sigma_{i,i} = \lambda_i$. U is an $N+1 \times N+1$ square matrix and its column is the eigenvector of V. In this case, U is also a unitary matrix. A suboptimal solution to (P4) can be written as $\bar{v}` = U\Sigma^{\frac{1}{2}} r$, where $r \in \mathbb{C}^{(N+1)\times 1}$ is a random vector generated according to $r \in \mathcal{C}N(0, I_{N+1})$ with $\mathcal{C}N(0, I_{N+1})$. Finally, we need to subtract the phase effect of the newly introduced variable t. The solution v to problem (P3) can be recovered by $v = e^{j \arg([\frac{\bar{v}`}{\bar{v}`_{N+1}}]_{(1:N)})}$, where (1:N) represents the first N elements.

After determining the phase of RIS, we search the optimal allocation of P1 and P2, which makes E_3 maximum.

4. Simulation Result

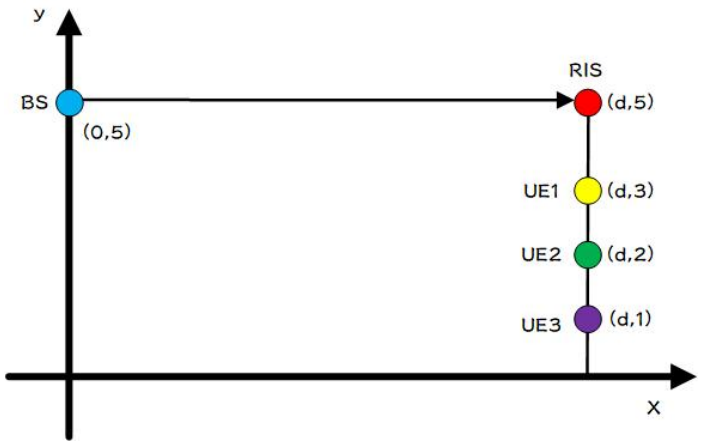

Fig. 2. Simulation model

As shown in Fig. 2, we consider a communication scenario where the RIS and UE 1, UE 2, UE 3 are on the same vertical line, and the base station is $d_0 = 100m$ away, while the vertical distance between RIS and UE 1 is 2m, and the vertical distance between UE 1, UE 2, UE 3 is 1m. The height of the base station is $d_{v0} = 5m$, and the height of the UE1 is $d_{v1} = 1m$. Correspondingly, the BS-UE 1 link distance are given by $d = \sqrt{d_0^2 + (d_{v0} - d_{v1})^2}$. During transmission, we model the channel according to the following equation: $|H|^2 = d^{loss} * noise_{ref}$. The parameters in our model are shown in the following table:

TABLE I. SIMULATION PARAMETER

Parameter	Value
Transmitted power	100W
Channel loss	-2.2
SINR for UE 1 and UE 2	10dB
Reference noise	10^{-3}
Bandwidth	10MHz
Noise power spectral density	$3.9810717055\times 10^{-21}$

Fig. 3 shows that we have a significant gain in the received E_3 with the assistance of RIS compared to the case without RIS. At 40 W, N=50, E_3=2.04 μW. When the transmitting power is increased to 50 W, E_3=2.58 μW, an increase of 0.5 μW, basically every 10 W increase received power by 0.5 μW to 1 μW. Increasing the number of reflecting surface units leads to a higher received power when the transmit power is constant. When the power P = 100W, the received power will be 6.26 μW for 80 elements, and it will increase to 5.34 μW and 4.83 μW as N increases. Therefore, a larger reflector unit N will bring more received power. RIS with 80 units can receive the same power as conventional solutions, while saving 20W transmit power.

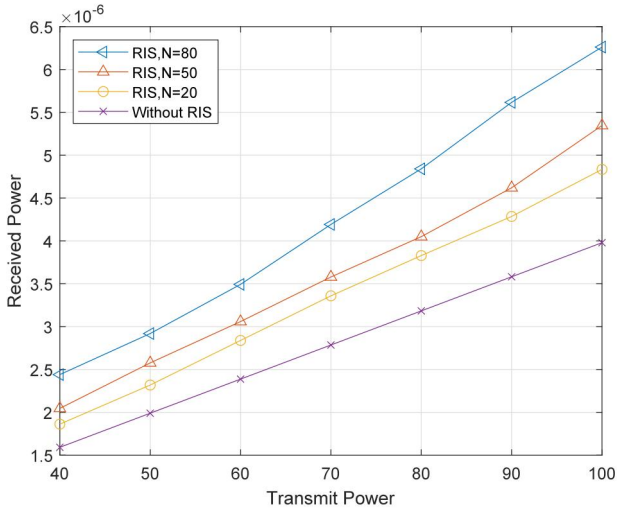

Fig. 3. Received power verses transmitted power

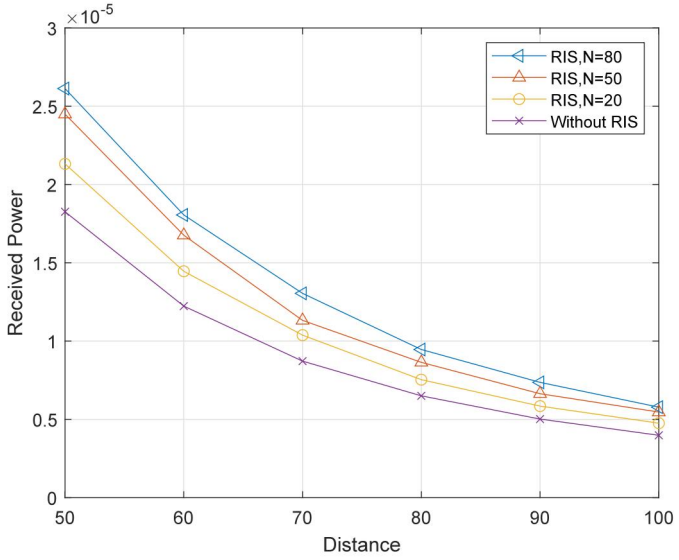

Fig. 4. Received power verses the distance between BS and RIS

In Fig. 4, we consider the relationship between the distance d and our goal E_3. This is because longer distances mean stronger attenuation, and eventually the received E_3 decreases as d increases. It can be noted that as the distance increases, our proposed scheme always receives more energy compared to the system without RIS. When the RIS has 80 reflective units, the RIS can obtain the same acceptance capacity as conventional solutions from 20 meters away. The practical application value of RIS is evident as it significantly enhances the working distance of user equipment. At d = 50, the received power is: 26μW,24 μW and 21 μW as N increases. The traditional system receives 18 μW under the same circumstance. RIS performance is very good at distances d between 50 and 70, and the closer the distance the better the performance of RIS.

In Fig. 5, we compare the received E_3 versus channel loss at N=30, 50, 80. First, the performance with and without RIS is very similar when the channel loss is relatively large. This is because the signal is very weak after a distance of 100, and RIS does not amplify the signal, but only adjusts the phase of the signal, so the advantage is not obvious when the loss is large. The more reflecting elements, the higher E_3. In the case of -2.2 channel loss, as N increases, the received power is 6.26 μW, 5.34 μW and 4.83 μW, respectively. Compared to the case without RIS assistance E_3 = 3.97 μW, the received power is improved by 1 μW. In addition, since the road loss exists in the problem as an exponential function, the relationship between loss and E_3 roughly takes the form of an exponential function, which is consistent with the theory.

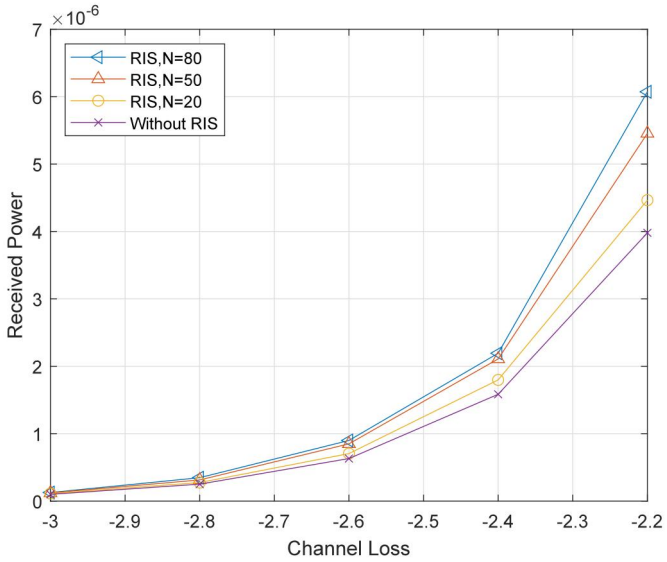

Fig. 5. Received power verses channel loss

The exceptional EH results are credited to the substantial increase in received energy at UE 3 due to RIS, as well as the guarantee of sufficient SINR for both UE 1 and UE 2.

5. Conclusion

In this paper, we used RIS to complement the NOMA-based SWIPT system and found through simulations that our scheme improved the efficiency of energy transmission compared to the conventional approach without RIS. Based on our simulations of parameters such as reflective units and propagation losses, we found that increasing the number of reflective units and reducing the distance and path loss can significantly improve the efficiency of energy transmission while ensuring the service quality of UE 1 and UE 2.

References

[1] B. Li, F. Si, D. Han and W. Wu, "IRS-aided SWIPT systems with power splitting and artificial noise," China Communications, vol. 19, no. 4, pp. 108-120, April 2022.

[2] Z. Yang and Y. Zhang, "Optimal SWIPT in RIS-Aided MIMO Networks," IEEE Access, vol. 9, pp. 112552-112560, 2021.

[3] W. Lu, Y . Gong, J. Wu, H. Peng, and J. Hua, ‘‘Simultaneous wireless information and power transfer based on joint subcarrier and power allocation in OFDM systems,’’ IEEE Access, vol. 5, pp. 2763–2770, 2017.

[4] W. Wang, R. Wang, H. Mehrpouyan, N. Zhao, and G. Zhang, ‘‘Beamforming for simultaneous wireless information and power transfer in two-way relay channels,’’ IEEE Access, vol. 5, pp. 9235–9250, 2017.

[5] Y. Huang, M. Liu and Y. Liu, "Energy-Efficient SWIPT in IoT Distributed Antenna Systems," IEEE Internet of Things Journal, vol. 5, no. 4, pp. 2646-2656, Aug. 2018.

[6] A. Jehan and M. Zeeshan, "Comparative Performance Analysis of Code-Domain NOMA and Power-Domain NOMA," 2022 16th International Conference on Ubiquitous Information Management and Communication (IMCOM), Seoul, Korea, Republic of, 2022, pp. 1-6.

[7] J. Zhang, L. Zhu, Z. Xiao, X. Cao, D. O. Wu and X. -G. Xia, "Optimal and Sub-Optimal Uplink NOMA: Joint User Grouping, Decoding Order, and Power Control," IEEE Wireless Communications Letters, vol. 9, no. 2, pp. 254-257, Feb. 2020, doi: 10.1109/LWC.2019.2951765.

[8] H. Zhang, F. Fang, J. Cheng, K. Long, W. Wang, and V . C. M. Leung,“Energy-efficient resource allocation in NOMA heterogeneous networks,”IEEE Wireless Communication., vol. 25, no. 2, pp. 48–53, Apr. 2018.

[9] V. Degli-Esposti, E. M. Vitucci, M. D. Renzo and S. A. Tretyakov, "Reradiation and Scattering From a Reconfigurable Intelligent Surface: A General Macroscopic Model," IEEE Transactions on Antennas and Propagation, vol. 70, no. 10, pp. 8691-8706, Oct. 2022.

[10] J. Zuo, Y. Liu, Z. Qin and N. Al-Dhahir, "Resource Allocation in Intelligent Reflecting Surface Assisted NOMA Systems," IEEE Transactions on Communications, vol. 68, no. 11, pp. 7170-7183, Nov. 2020.

[11] Q. Wu and R. Zhang, "Intelligent Reflecting Surface Enhanced Wireless Network via Joint Active and Passive Beamforming," IEEE Transactions on Wireless Communications, vol. 18, no. 11, pp. 5394-5409, Nov. 2019.

[12] E. Björnson, Ö. Özdogan and E. G. Larsson, "Intelligent Reflecting Surface Versus Decode-and-Forward: How Large Surfaces are Needed to Beat Relaying?" IEEE Wireless Communications Letters, vol. 9, no. 2, pp. 244-248, Feb. 2020.

[13] Q. Liu, M. Lu, N. Li, M. Li, F. Li and Z. Zhang, "Joint Beamforming and Power Splitting Optimization for RIS-Assited Cooperative SWIPT NOMA Systems," 2022 IEEE Wireless Communications and Networking Conference (WCNC), 2022, pp. 351-356.

[14] M. Diamanti, E. E. Tsiropoulou and S. Papavassiliou, "The Joint Power of NOMA and Reconfigurable Intelligent Surfaces in SWIPT Networks," 2021 IEEE 22nd International Workshop on Signal Processing Advances in Wireless Communications (SPAWC), 2021, pp. 621-625.

[15] Q. Wu and R. Zhang, "Weighted Sum Power Maximization for Intelligent Reflecting Surface Aided SWIPT," IEEE Wireless Communications Letters, vol. 9, no. 5, pp. 586-590, May 2020.

[16] J. Ren, X. Lei, Z. Peng, X. Tang and O. A. Dobre, "RIS-Assisted Cooperative NOMA With SWIPT," IEEE Wireless Communications Letters, vol. 12, no. 3, pp. 446-450, March 2023.

[17] J. D. Griffin and G. D. Durgin, “Complete link budgets for backscatter-radio and RFID systems,” IEEE Antennas Propag. Mag., vol. 51, no. 2,Apr. 2009.

[18] M. Grant and S. Boyd, “CVX: MATLAB software for disciplined convex programming,” 2016. [Online] Available: http://cvxr.com/cvx.

[19] Q. Wu and R. Zhang, "Intelligent Reflecting Surface Enhanced Wireless Network: Joint Active and Passive Beamforming Design," 2018 IEEE Global Communications Conference (GLOBECOM), Abu Dhabi, United Arab Emirates, 2018, pp. 1-6.